

Viscoelastic Material Properties of the Peripapillary Sclera in Normal and Early-Glaucoma Monkey Eyes

J. Crawford Downs,^{1,2} J-K. Francis Suh,² Kevin A. Thomas,³ Anthony J. Bellezza,¹ Richard T. Hart,² and Claude F. Burgoyne^{1,2}

PURPOSE. To test the hypothesis that changes in the viscoelastic material properties of peripapillary sclera are present within monkey eyes at the onset of early experimental glaucoma detected by confocal scanning laser tomography (CSLT).

METHODS. Short-term (3–9 weeks), moderate (≤ 44 mm Hg) intraocular pressure (IOP) elevation was induced in one eye of each of eight male monkeys by laserizing the trabecular meshwork. This procedure generated early experimental glaucoma, defined as the onset of CSLT-detected optic nerve head (ONH) surface change, in the treated eye. Scleral tensile specimens from the superior and inferior quadrants of the eight early-glaucoma eyes were subjected to uniaxial stress relaxation and tensile tests to failure and the results compared with similar data obtained in a previous study of 12 normal (nonglaucomatous) eyes. Linear viscoelastic theory was used to characterize viscoelastic material property parameters for each specimen. Differences in each parameter due to quadrant and treatment were assessed by analysis of variance (ANOVA).

RESULTS. Peripapillary sclera from the early-glaucoma eyes exhibited an equilibrium modulus (7.46 ± 1.58 MPa) that was significantly greater than that measured in normal eyes (4.94 ± 1.22 MPa; mean \pm 95% confidence interval, $P < 0.01$, ANOVA). Quadrant differences were not significant for the viscoelastic parameters within each treatment group.

CONCLUSIONS. The long-term viscoelastic material properties of monkey peripapillary sclera are altered by exposure to moderate, short-term, chronic IOP elevations and these alterations are present at the onset of CSLT-detected glaucomatous damage to the ONH. Damage to and/or remodeling of the extracellular matrix of these tissues may underlie these changes in scleral material properties. (*Invest Ophthalmol Vis Sci.* 2005;46:540–546) DOI:10.1167/iovs.04-0114

From the ¹LSU Eye Center and the ³Department of Orthopaedic Surgery, Louisiana State University Health Sciences Center, New Orleans, Louisiana; and the ²Department of Biomedical Engineering, Tulane University, New Orleans, Louisiana.

Presented in part at the annual meeting of the Association for Research in Vision and Ophthalmology, Fort Lauderdale, Florida, May 2001.

Supported in part by Grants R01EY011610 (CFB) and P30EY002377 (departmental core grant) from the National Eye Institute; a grant from The Whitaker Foundation, Arlington, Virginia (CFB); and a Career Development Award (CFB) and an unrestricted departmental grant (LSU Eye Center) from Research to Prevent Blindness, Inc., New York, New York.

Submitted for publication February 5, 2004; revised July 19, 2004; accepted August 16, 2004.

Disclosure: J.C. Downs, None; J-K.F. Suh, None; K.A. Thomas, None; A.J. Bellezza, None; R.T. Hart, None; C.F. Burgoyne, None

The publication costs of this article were defrayed in part by page charge payment. This article must therefore be marked "advertisement" in accordance with 18 U.S.C. §1734 solely to indicate this fact.

Corresponding author: J. Crawford Downs, LSU Eye Center, 2020 Gravier Street, Suite B, New Orleans, LA 70112; jdowns@lsuhsc.edu.

We are constructing finite element models of the load-bearing connective tissues of the monkey optic nerve head (ONH) and posterior scleral shell as part of our ongoing studies of the optic nerve head as a biomechanical structure (Bellezza AJ, et al. *IOVS* 2003;44:ARVO E-Abstract 1094; Downs JC, et al. *IOVS* 2002;43:ARVO E-Abstract 4042).¹ The finite element method is a computer-based engineering technique that estimates the stresses (force/cross-sectional area) and strains (local deformation under those stresses) within a complex load-bearing structure.² The important aspects of a finite element model are the three-dimensional geometry and material properties of the load-bearing structure and the appropriate boundary and mechanical loading conditions.² Within such models of the monkey ONH, scleral material properties are needed to characterize accurately the important transition between the peripapillary sclera and the peripheral laminar beams.

To characterize the material properties of peripapillary sclera, we constructed a controlled-environment testing apparatus capable of performing uniaxial biomechanical testing of soft tissues in tension. The overall response of a tissue to a load is the combination of instantaneous (elastic) and time-dependent (viscous) responses, which are governed by its viscoelastic material properties. All soft tissues are viscoelastic, and the characterization of the instantaneous and time-dependent aspects of these material properties is important in understanding a tissue's behavior as a load-bearing structure and its response to short- and long-term changes in the applied load. Accurate characterization of a tissue's material properties can lead to a broader understanding of the mechanisms that underlie tissue damage, as well as determine the resultant altered load-bearing behavior of a remodeled or healed tissue.

In a previous report we performed quadrant-based uniaxial tensile testing of peripapillary sclera from normal rabbit and normal monkey eyes³ and found no differences in the viscoelastic material properties of the peripapillary sclera by quadrant (superior, inferior, nasal, and temporal to the ONH) in either species. In addition, when normal rabbit and monkey sclera were compared with one another, peripapillary sclera from monkey eyes was stiffer and showed slower stress relaxation than sclera from rabbit eyes.

The present study tests the hypothesis that changes in the viscoelastic material properties of monkey peripapillary sclera are present at the earliest detectable stage of glaucomatous damage to the ONH, defined as the onset of confocal scanning laser tomography (CSLT)-detected ONH surface change.

MATERIALS AND METHODS

Animals, Scleral Specimens, and Study Design

All animals were treated in accordance with the ARVO Statement for the Use of Animals in Ophthalmic and Vision Research. In the present study, a single scleral tensile specimen was generated from either the superior or inferior quadrant of eight eyes with experimental early glaucoma, yielding four early-glaucoma specimens for each quadrant. Each specimen underwent a multistage uniaxial tensile test. Viscoelas-

tic material property parameters for each early-glaucoma specimen were then calculated, and the data were pooled by quadrant and compared by analysis of variance (ANOVA) with the superior and inferior quadrant data obtained from 12 normal eyes in a previous study.³ Thus, this report contains viscoelastic material property data for peripapillary scleral specimens from 20 eyes of 14 monkeys: 8 early-glaucoma eyes (specimens 1–8) and 12 normal eyes (specimens 9–20; Table 1).

Early Experimental Glaucoma

Our protocol for generating early experimental glaucoma has been described in detail in a previous report.⁴ Briefly, in both eyes of eight monkeys, compliance testing of the ONH surface was performed on three separate occasions to characterize normal ONH surface position and compliance. Early experimental glaucoma was then induced in one eye of each animal by lasering the trabecular meshwork every 2 weeks until a statistically significant elevation in IOP was observed (mean \pm SD of the IOP elevation, 19 ± 7.2 mm Hg). Each eye was compliance tested every 2 weeks from the beginning of lasering to detect the onset of early glaucomatous damage to the ONH tissues, defined as the onset of fixed posterior deformation of the ONH surface and/or the onset of ONH surface hypercompliance in two consecutive compliance tests.⁴

Specimen Preparation and General Testing Methodology

Our methodology, which was described in detail in our previous report,³ is briefly presented here. Each animal was anesthetized with an intramuscular injection of ketamine/xylazine and killed with an intravenous injection of pentobarbital. Immediately after death, each eye was enucleated and cleaned of all extraorbital tissues. The ONH was removed from the surrounding sclera with a 6-mm-diameter trephine for use in another study, with care taken to include as little of the peripapillary sclera in the testing quadrant as possible (typically, ≤ 1 mm). A dumbbell-shaped cutting die was used to produce a precise tensile specimen of peripapillary sclera with a gauge length of 8 mm, a gauge width of 3 mm, and grip-end widths of 7 mm. Before testing, the scleral specimens were stored in isotonic (pH 7.4) phosphate-buffered saline (PBS) for a minimum of 30 minutes at zero load to allow for equilibration and rehydration of the tissues.

Each scleral tensile specimen was clamped into custom-built, soft-tissue grips and mounted in a testing environment chamber. The custom-built chamber was designed to maintain the specimen in a fog of 37°C PBS for the duration of each testing sequence. The chamber was mounted on a servo-hydraulic test frame (Bionix 858; MTS, Inc., Eden Prairie, MN), fitted with an integrated computer-based test controller and digital data acquisition system (Teststar II; MTS, Inc.). A biomedical extensometer (model 632.32F; MTS, Inc.) and a 250-N load cell (in the 10% range, 0–25 N; model 661.11A; MTS, Inc.) were used to measure strain and load, respectively.

Uniaxial Testing in Tension

Peripapillary scleral specimens were tested as follows, using a protocol identical with that reported previously.³ The specimen was fitted in the testing chamber and warmed to 37°C in a fog of PBS at zero load for approximately 15 minutes. After an 0.08-N tensile preload was applied and the extensometer was mounted, the specimen was initially preconditioned with 10 cycles of 0 to 150 μ m of grip-to-grip displacement at a rate of 150 μ m/s in displacement control, followed by a 360-second recovery period at zero displacement. The specimen was then subjected to a second preconditioning phase consisting of 10 cycles of 50- to 350- μ m displacement at 175 μ m/s and rested again for 360 seconds. The second phase of preconditioning generated strain amplitudes of approximately 1% in the central 5-mm gauge section, and was performed to provide a cyclic loading regimen that could be used for validation of future computational models of scleral tensile specimens. The specimen was then subjected to a stress relaxation test

consisting of a tensile ramp in strain rate control at a strain rate of 1% per second to 1% strain, with the ramp-ending displacement held for 1000 seconds. After a third 360-second recovery period at zero displacement, each specimen was subjected to a tensile ramp to failure (or a maximum of 20% strain) at a strain rate of 1%/s. Data for tensile load and gauge strain were recorded at 0.01-second intervals.

Estimation of Elastic and Viscoelastic Parameters for Each Specimen

Four principal viscoelastic parameters were derived from the stress relaxation test of each scleral tensile specimen. The *instantaneous modulus*, E_{0+} , is a measure of the instantaneous stiffness of the tissue. The *short-term* and *long-term time constants*, τ_S and τ_L , describe the time-dependent stress relaxation response of the sclera and are measures of how quickly the tissue relaxes to an equilibrium stress after a rapid deformation (Fig. 1). The short- and long-term time constants are measures of the shortest and longest time-scale components, respectively, of the tissue's stress relaxation response. The *equilibrium modulus*, E_∞ , is a measure of the tissue's stiffness after it has fully relaxed after a rapid deformation (Fig. 1) and is a measure of the long-term stiffness of the tissue. The full derivation of these parameters, which is described in our previous report,³ is briefly described in the next section.

Analytical Methods

Linear viscoelastic theory,⁵ incorporating a reduced relaxation function,^{6,7} was used to characterize the viscoelastic properties of peripapillary sclera as follows. A viscoelastic material, when subjected to a step strain input, ϵ_A , exhibits a stress relaxation response, σ , that can be expressed as

$$\sigma(\epsilon_A, t) = G(t)\sigma^e(\epsilon_A) \quad (1)$$

where $\sigma^e(\epsilon_A)$ is the linear elastic stress response defined at equilibrium (time, $t = \infty$) and $G(t)$ is the time-dependent, reduced-relaxation function that satisfies $G(\infty) = 1$.

We used the following functional form to define a spectral reduced-relaxation function

$$G(t) = \frac{c}{n} \sum_{i=1}^n e^{-t/\tau_i} + 1, \quad (2)$$

where c is the spectral magnitude, n is the number of spectral time constants, and $\tau_1 = \tau_S$ and $\tau_n = \tau_L$ are the short- and long-term relaxation time constants, respectively. Stress was normalized with respect to $\sigma(t = \infty)$ and we used Hooke's law as it applies to the fully relaxed state: $\sigma(\infty) = E_\infty \epsilon(\infty)$, where E_∞ is Young's modulus at equilibrium (equilibrium modulus). For given short- and long-term relaxation time constants, τ_S and τ_L , n spectral relaxation time constants were uniquely determined⁷ by the formula

$$\tau_i = e^{[\log(\tau_S) + (i-1)\Delta\tau]} \text{ for } i = 1, 2, \dots, n, \quad (3)$$

where $\Delta\tau = \frac{\log(\tau_L) - \log(\tau_S)}{(n-1)}$,

which distributes the spectral time constants at equal intervals between τ_S and τ_L on the log time scale. We calculated the instantaneous modulus of the tissue, $E_{0+} = \sigma(0)/\epsilon_0$, by evaluating equation 1 at time, $t = 0^+$.

For a linear increase in strain at a finite rate, $\dot{\epsilon}$, beginning at time 0 and ending at time t_0 , the stress at time, t , according to equations 1, 2 and 3 is

$$\sigma(t) = \dot{\epsilon} E_\infty \left[\frac{c}{n} \sum_{i=1}^n \tau_i (1 - e^{-t/\tau_i}) + t \right] \text{ for } 0 \leq t \leq t_0, \quad (4)$$

TABLE 1. Tensile Specimen, Study Eye, and Animal Data

Tensile Specimen Number	Monkey ID	Tested Quadrant	Condition at Death	Eye	Species	Weight (kg)	Age (y)	IOP (mm Hg)		Estimated Duration of IOP Elevation (wk)	Axial Length (mm) (IOP = 10 mm Hg)	
								Normal (Pre-laser)	Maximum (Post-laser)		Normal	Before Death*
Early glaucoma eyes												
1	2J	Superior	EG	Left	Rhesus	5.7	5.5	8	26	4	20.0	20.5
2	2N	Inferior	EG	Left	Rhesus	6.5	6.2	12	24	6	19.9	20.2
3	2R	Superior	EG	Right	Cynomolgus	4.7	5.8	9	25	4	19.0	19.1
4	2S	Inferior	EG	Right	Cynomolgus	5.3	7.0	8	32	6	18.1	18.6
5	2T	Inferior	EG	Left	Cynomolgus	7.2	7.0	8	25	7	19.4	20.1
6	2U	Superior	EG	Left	Cynomolgus	5.4	5.8	9	30	4	18.8	19.0
7	2V	Superior	EG	Left	Cynomolgus	7.9	N/A	8	20	3	19.0	19.6
8	2Y	Inferior	EG	Left	Cynomolgus	7.5	6.4	10	44	9	18.9	19.7
Normal eyes												
9	2J	Superior	Normal	Right	Rhesus	5.7	5.5	9	—	—	20.5	—
10	2K	Superior	Normal	Left	Rhesus	4.3	3.1	NA	—	—	NA	—
11	2L	Inferior	Normal	Right	Rhesus	5.1	4.5	NA	—	—	NA	—
12	2M	Inferior	Normal	Right	Rhesus	5.4	5.7	NA	—	—	NA	—
13	2M	Inferior	Normal	Left	Rhesus	5.4	5.7	NA	—	—	NA	—
14	2N	Inferior	Normal	Right	Rhesus	6.5	6.2	13	—	—	19.9	—
15	2O	Superior	Normal	Right	Rhesus	6.6	6.7	NA	—	—	NA	—
16	2O	Superior	Normal	Left	Rhesus	6.6	6.7	NA	—	—	NA	—
17	2Q	Superior	Normal	Left	Rhesus	6.3	4.3	NA	—	—	NA	—
18	2S	Superior	Normal	Left	Cynomolgus	5.3	7.0	8	—	—	18.1	—
19	2W	Inferior	Normal	Right	Cynomolgus	6.5	NA	NA	—	—	NA	—
20	2Y	Inferior	Normal	Right	Cynomolgus	7.5	6.4	10	—	—	19.1	—

EG, early glaucoma; NA, not available.

* Axial length measure taken during final compliance testing session using Ascan ultrasonography (model A-1500; Sonomed, Lake Success, NY).

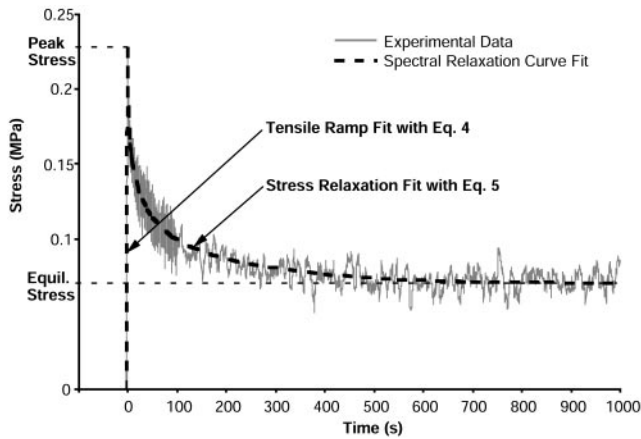


FIGURE 1. Graph of the experimental data and associated curve fit showing the tensile ramp and relaxation phases of the stress relaxation test of a representative specimen.

$$\sigma(t) = \dot{\epsilon} E_{\infty} \left[\frac{c}{n} \sum_{i=1}^n \tau_i (e^{t/\tau_i} - 1) e^{-t/\tau_i} + t_0 \right] \text{ for } t_0 \leq t. \quad (5)$$

Equations 4 and 5 were fit simultaneously to the two stages of the experimental stress relaxation data⁶ (the tensile ramp and the relaxation phase), by using the Levenberg-Marquardt nonlinear, least-squares algorithm, which yields unique estimates⁷ of c , τ_S , τ_L , and E_{∞} for a given value of n (Fig. 1).

For a sufficiently large n , the parameters c , τ_S , and τ_L in the spectral relaxation function defined by equations 2 and 3 are equivalent to Fung's well-known reduced-relaxation function,^{3,5,7} and c , τ_S , and τ_L can be uniquely defined independent of n .⁷ Chi-squared (χ^2 , a measure of goodness of fit) was minimized to determine the minimum value of n necessary to guarantee the uniqueness of these parameters.³ The minimum n required for the parameters to converge to their unique, terminal values varied from 3 to 7, depending on the specimen. No significant change in the parameters resulted from increasing the number of spectral terms beyond that necessary to minimize χ^2 .

Statistical Analysis

Viscoelastic Parameters. An ANOVA was used to determine the effects of quadrant and treatment on the short- and long-term time constants, and the instantaneous and equilibrium moduli. Confidence intervals were calculated using the SE, which employs the pooled variance of all values in the ANOVA for each parameter.

Tensile Ramp to Failure Testing. A second ANOVA was used to assess the effects of quadrant and treatment on the stress values obtained at the integer percentage values of strain (1%, 2%, . . . , 10%) for the tensile ramp-to-failure tests.

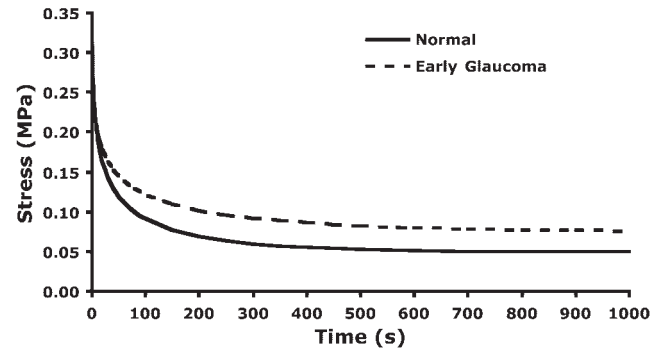


FIGURE 2. Mean stress relaxation responses of peripapillary sclera from normal and early-glaucoma monkey eyes (superior and inferior quadrant specimens combined). Note that the curves diverged only after approximately 120 seconds of loading. See Table 2 for a statistical comparison of the parameters used to generate these curves.

RESULTS

Data for the 8 early-glaucoma and 12 normal peripapillary scleral specimens are summarized in Table 2. Because the material properties by quadrant (superior and inferior only) within each treatment group (normal and early glaucoma) were not different ($P > 0.05$, ANOVA), the data for each parameter are reported by treatment group only.

Viscoelastic Material Property Parameters by Treatment Group

The instantaneous modulus and the long- and short-term time constants of peripapillary sclera from the superior and inferior quadrants of normal ($n = 12$) and early-glaucoma ($n = 8$) monkey eyes were not significantly different by treatment group ($P > 0.05$, ANOVA; Table 2). However, the equilibrium modulus of sclera from early-glaucoma eyes (7.46 ± 1.58 MPa) was significantly higher than that from normal eyes (4.94 ± 1.22 MPa; Table 2, $P < 0.01$, ANOVA).

The mean stress relaxation responses of peripapillary sclera (superior and inferior quadrants pooled) from both normal and early-glaucoma monkey eyes are shown in Figure 2. Note the high degree of stress relaxation over the relatively short duration of the test and the higher equilibrium stress evident in the early-glaucoma group, which is a manifestation of the significantly higher equilibrium modulus in the early-glaucoma eyes.

Tensile Ramp to Failure by Treatment Group

Mean stress-strain curves for tensile ramps to failure at a strain rate of 1% per second to 10% strain are plotted by treatment group in Figure 3. These curves are virtually identical, which indicates that a detectable alteration in the short-term mechan-

TABLE 2. Viscoelastic Material Properties by Treatment Group

	Normal Eyes ($n = 12$)	Early-Glaucoma Eyes ($n = 8$)
Instantaneous modulus*, E_{0+} (MPa)	33.9 ± 3.43	34.3 ± 4.45
Short-term time constant, τ_S (s)	0.527 ± 0.271	0.717 ± 0.352
Long-term time constant, τ_L (s)	183 ± 82.2	252 ± 107
Equilibrium modulus, E_{∞} (MPa)	4.94 ± 1.22	$7.46 \pm 1.58†$

Data are the mean \pm 95% confidence interval.
 * $E_{0+} = [1 + c \ln(\tau_L/\tau_S)]E_{\infty}$.
 † Significantly different from the normal eyes ($P \leq 0.01$).

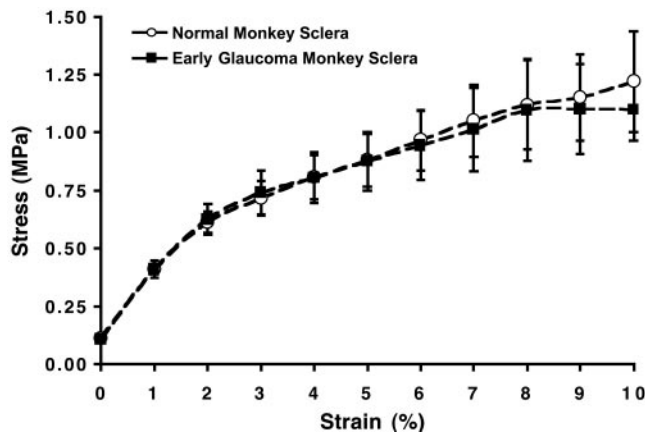


FIGURE 3. Mean stress-strain curves for peripapillary sclera from normal and early glaucoma monkey eyes tested in uniaxial tension at a strain rate of 1% per second (superior and inferior quadrant data only; bars, 95% confidence interval).

ical response of the tissues was not present in eyes with early experimental glaucoma.

DISCUSSION

In this study, we characterized the uniaxial viscoelastic material properties of peripapillary sclera from the superior and inferior quadrants of monkey eyes with early experimental glaucoma, to test the hypothesis that alterations in the peripapillary sclera of early-glaucoma monkey eyes occur early in response to chronic IOP elevation. To do so, we compared the peripapillary scleral material properties from early-glaucoma eyes (determined in this study) with the material properties of peripapillary sclera from the superior and inferior quadrants of normal monkey eyes studied as part of a previous report.³ The testing protocol and the analytical approach were identical with those used in our previous work.³

The principal findings of the current report are as follows. First, peripapillary sclera (superior and inferior quadrants only) of early-glaucoma eyes exhibited an equilibrium modulus that was significantly greater than that measured in normal eyes ($P < 0.01$, ANOVA). Second, we detected no differences between peripapillary sclera from early-glaucoma and normal eyes in the instantaneous modulus and the short- and long-term time constants ($P > 0.05$, ANOVA). This finding suggests that the long-term elastic properties of monkey peripapillary sclera are altered by exposure to moderate (23–44 mm Hg), short-term (3–9 weeks), chronic IOP elevations and that these alterations are present at the onset of CSLT-detected glaucomatous damage⁴ to the ONH. Third, we detected no differences in the viscoelastic material properties of peripapillary sclera from the superior and inferior quadrants of early-glaucoma eyes. Finally, stress-strain curves from a tensile test to failure at a 1% per second strain rate were virtually identical in sclera from both normal and early-glaucoma eyes.

For the material properties of peripapillary sclera to be altered at this early stage of glaucomatous damage, the extracellular matrix (ECM) of the tissue must be damaged and/or remodeled. Cellular mechanotransduction and ECM remodeling have been reported in other load-bearing collagenous tissues, in which fibroblasts secrete factors that elicit changes in the surrounding ECM in response to an increase in strain.⁸ It is likely that such strain-induced changes in protein and genetic factor expression act to increase the resistance of the ECM to further strain, thereby shielding the tissues and cells from future damage. Changes in the ECM of the lamina cribrosa in

glaucomatous human and monkey eyes with more advanced glaucomatous damage have been reported by other investigators.^{9–12} Quigley et al.¹³ reported a decrease in collagen fibril density within the lamina cribrosa and peripapillary sclera in human eyes with moderate or severe glaucomatous damage. Although their study did not detect this effect in monkeys, our results indicate that alterations in the ECM of peripapillary sclera occur early in response to chronic IOP elevation and that these alterations are sufficiently large to be detected using mechanical testing.

Although IOP-related stress remains constant across eyes with identical peripapillary geometry (thickness and curvature), strain (local deformation) within sclera that is identically loaded depends on the sclera's material properties. Once the material properties of the peripapillary sclera are altered, the eye deforms differently under the same level of IOP-related stress. IOP-induced deformation within the peripapillary sclera should be an important contributing factor to the overall biomechanical response of the ONH. Peripapillary scleral deformation may be directly transferred to the peripheral laminar insertions through the scleral canal wall. Large scleral deformations may secondarily diminish the volume flow of blood through the contained branches of the posterior ciliary arteries.¹⁴ In addition, in those conditions, such as myopia, in which either the sclera is thinned^{15,16} or its ECM altered,¹⁷ scleral deformation after a similar change in IOP is likely to be increased.

We recently reported that posterior sclera of young adult monkeys thins in response to exposure to chronic IOP elevations,¹⁸ and this may also hold true for peripapillary sclera. If sclera from early-glaucoma eyes is thinner than sclera from normal eyes, then the scleral stress would be higher in the early-glaucoma eyes at a given IOP. With respect to the testing reported herein, this phenomenon would result in an increase in the instantaneous and equilibrium moduli we report in the early-glaucoma eyes, thereby accentuating the difference in the equilibrium modulus.

In physical terms, the increased equilibrium modulus that we report indicates that peripapillary sclera from early-glaucoma eyes is stiffer than that from normal eyes for IOP increases that last longer than 2 minutes (Fig. 2). A stiffer scleral shell stretches less at a given elevated IOP and is thus less able to reduce IOP over time through globe expansion. Hence, after an IOP elevation of fixed magnitude lasting longer than 2 minutes (such as diurnal IOP fluctuations), IOP remains higher in an early-glaucoma eye than in a normal eye (Fig. 2). However, this phenomenon would not be present during transient IOP elevations (blink, squint, or eye rub; Figs. 2, 3), the response to which is largely dependent on the instantaneous modulus and short- and long-term time constants, parameters that exhibited no detectable difference by treatment. The virtually identical stress-strain curves plotted in Figure 3 confirm that the instantaneous elastic properties of sclera are not detectably altered in response to chronic IOP elevation.

Zeimer¹⁹ has suggested that a mismatch of the material properties of the lamina cribrosa and peripapillary sclera is an important contributor to the pathophysiology of glaucomatous damage to the tissues of the ONH. We have reported that hypercompliance of the ONH surface^{4,20,21} and underlying connective tissues⁴ is present at the same stage of early glaucomatous damage reported in the current study. If the ONH connective tissues have become more compliant and the peripapillary sclera less compliant in an eye with early glaucoma, IOP elevations (such as diurnal IOP fluctuations) may expose the glaucomatous ONH to higher shear stresses at the insertion of the lamina cribrosa into the sclera.

Our study is limited by the following considerations. First, due to the size of the harvested specimens and the nature of

tensile testing, we could generate only one peripapillary scleral tensile specimen and one measurement of each of the material property parameters per eye. Thus, due to the lack of repeated measures, we were not able to directly compare the material properties of the peripapillary sclera from the normal and early-glaucoma eyes within individual monkeys.

Second, only eight early-glaucoma eyes were generated in this study, and so we were limited to testing specimens from the superior and inferior quadrants to maintain an adequate sample size of $n = 4$ per quadrant. Peripapillary scleral material properties of specimens from the nasal and temporal quadrants may be altered differently as a result of exposure to IOP elevations, compared with the superior and inferior quadrant data reported here. Future studies are necessary to characterize the peripapillary sclera fully at this early stage of connective tissue damage.

The limitations of the testing methodology have been described in detail³ and are recounted briefly here. First, we did not measure thickness within each specimen, but instead assigned a thickness of 400 μm to all our specimens based on our previous characterization of monkey peripapillary scleral thickness.²² The specimens were taken beginning approximately 1 mm from the scleral canal, which is outside the region of greatest variability in peripapillary scleral thickness.²² We were unable to measure scleral thickness with ultrasound or other nondestructive techniques, as it is not possible to distinguish the load-bearing sclera from the adjacent episclera in fresh tissues. Assigning a fixed scleral thickness for the calculation of stress is a major assumption and is a likely source of error in the reported results, although previous work has shown no statistically significant differences in the thickness of sclera from the superior and inferior quadrants in the peripapillary region.²² That the inferior and superior quadrants exhibit similar material properties suggests that there is little difference in scleral thickness between quadrants within treatment groups. Also, the nearly identical short-term stress-strain response of sclera from normal and early-glaucoma eyes (Fig. 3) and the lack of significant treatment effect in the instantaneous modulus and time constants (Table 2) suggest that scleral thickness did not vary significantly between treatment groups in this study. It is possible that sclera from the glaucomatous eyes is thinner and stiffer than sclera from normal eyes, resulting in the similar instantaneous responses we report, but that would only accentuate the reported difference in equilibrium modulus.

Second, the preload necessary to assure consistent mounting of the extensometer arms (0.08 N) generated scleral stresses that are relatively high compared with normal levels of IOP. Using this type of contact extensometer was necessary to employ strain-rate-controlled testing. A uniaxial tensile preload of 0.08 N is equivalent to an IOP of approximately 40 mm Hg.²³ This is higher than the IOPs of 8 to 18 mm Hg we measured in the normal eyes of resting, anesthetized monkeys (Table 1).

Third, uniaxial tensile testing was used to ascertain the isotropic (uniform) properties of an anisotropic (nonuniform) tissue. Sclera is likely to be stiffer in the direction of the predominant collagen fibril orientation, which depends on location in the globe. Our assumption of isotropic properties is based on previous work on fibril orientation in the peripapillary region, where the fibrils follow a circular path ringing the scleral canal.^{13,15,24-26} Uniaxial testing of tensile specimens from the peripapillary region should provide a valid first estimate of the material properties of sclera in the axial direction of the specimen, which coincides with the direction of predominant fiber orientation. The moduli of sclera in any direc-

tion not parallel to that of the predominant fibril orientation are likely to be lower than that reported here.

Finally, it should be noted that the early-glaucoma specimens were predominantly from cynomolgus monkeys and the normal specimens were predominantly from rhesus monkeys (Table 1). This was inadvertent and may be a source of error if there are species-specific differences in peripapillary scleral material properties. We performed an ANOVA to compare the viscoelastic properties of inferior scleral tensile specimens 11 to 14 (rhesus) to that of specimens 19 and 20 (cynomolgus; Table 1), and found no significant differences in any of the parameters by species (data not shown).

The uniaxial viscoelastic material properties reported in Table 2 are being incorporated into finite element models of the posterior scleral shell and ONH of the normal and early-glaucoma monkey to study the role of IOP in the development and progression of glaucoma (Bellezza AJ, et al. *IOVS* 2003;44:ARVO E-Abstract 1094; Downs JC, et al. *IOVS* 2002;43:ARVO E-Abstract 4042). Future improvements in testing will allow us to generate biaxially determined anisotropic material properties of the sclera and incorporate these refined properties into our models.

References

- Bellezza AJ, Hart RT, Burgoyne CF. The optic nerve head as a biomechanical structure: initial finite element modeling. *Invest Ophthalmol Vis Sci.* 2000;41:2991-3000.
- Cook RD, Malkus DS, Plesha ME. *Concepts and Applications of Finite Element Analysis.* 3rd ed. New York: John Wiley & Sons; 1989.
- Downs JC, Suh J-KF, Thomas KA, Bellezza AJ, Burgoyne CF, Hart RT. Viscoelastic characterization of peripapillary sclera: material properties by quadrant in rabbit and monkey eyes. *J Biomech Eng.* 2003;125:124-131.
- Bellezza AJ, Rintalan CJ, Thompson HW, Downs JC, Hart RT, Burgoyne CF. Deformation of the lamina cribrosa and anterior scleral canal wall in early experimental glaucoma. *Invest Ophthalmol Vis Sci.* 2003;44:623-637.
- Fung YC. *Biomechanics: Mechanical Properties of Living Tissues.* 2nd ed. New York: Springer-Verlag; 1993.
- Kwan MK, Lin H-CL, Woo S-LY. On the viscoelastic properties of the anteromedial bundle of the anterior cruciate ligament. *J Biomech.* 1993;26:447-452.
- Suh J-KF, Bai S. Finite element formulation of biphasic poroviscoelastic model for articular cartilage. *J Biomech Eng.* 1998;120:195-201.
- Chiquet M, Matthisson M, Koch M, Tannheimer M, Chiquet-Ehrismann R. Regulation of extracellular matrix synthesis by mechanical stress. *Biochem Cell Biol.* 1996;74:737-744.
- Hernandez MR, Andrzejewska WM, Neufeld AH. Changes in the extracellular matrix of the human optic nerve head in primary open angle glaucoma. *Am J Ophthalmol.* 1990;109:180-188.
- Hernandez MR. Ultrastructural immunocytochemical analysis of elastin in the human lamina cribrosa: changes in elastic fibers in primary open angle glaucoma. *Invest Ophthalmol Vis Sci.* 1992;33:2891-2903.
- Pena JD, Agapova O, Gabelt BT, et al. Increased elastin expression in the astrocytes of the lamina cribrosa in response to elevated intraocular pressure. *Invest Ophthalmol Vis Sci.* 2001;42:2303-2314.
- Quigley HA, Addicks EM. Regional differences in the structure of the lamina cribrosa and their relation to glaucomatous optic nerve damage. *Arch Ophthalmol.* 1981;99:137-143.
- Quigley HA, Brown AE, Dorman-Pease ME. Alterations in elastin of the optic nerve head in human and experimental glaucoma. *Br J Ophthalmol.* 1991;75:552-557.
- Langham ME. The temporal relation between intraocular pressure and loss of vision in chronic simple glaucoma. *Glaucoma.* 1980;2:427-435.

15. Greene PR. Mechanical considerations of myopia: relative effects of accommodation, convergence, intraocular pressure, and the extraocular muscles. *Am J Optom Physiol Opt.* 1980;57:902-914.
16. Phillips JR, McBrien NA. Form deprivation myopia: elastic properties of sclera. *Ophthalmic Physiol Opt.* 1995;15:357-362.
17. McBrien NA, Moghaddam HO, Reeder AP, Moules S. Structural and biochemical changes in the sclera of experimentally myopic eyes. *Biochem Soc Trans.* 1991;19:861-865.
18. Downs JC, Ensor ME, Bellezza AJ, Thompson HW, Hart RT, Burgoyne CF. Posterior scleral thickness in perfusion-fixed normal and early-glaucoma monkey eyes. *Invest Ophthalmol Vis Sci.* 2001;42:3202-3208.
19. Zeimer R. Biomechanical properties of the optic nerve head. In: Drance SM, ed. *Optic Nerve Head in Glaucoma.* Amsterdam: Kugler Publications; 1995:107-121.
20. Burgoyne CF, Quigley HA, Thompson HW, Vitale S, Varma R. Early changes in optic disc compliance and surface position in experimental glaucoma. *Ophthalmology.* 1995;102:1800-1809.
21. Heickell AG, Bellezza AJ, Thompson HW, Burgoyne CF. Optic disc surface compliance testing using confocal scanning laser tomography in the normal monkey eye. *J Glaucoma.* 2001;10:369-382.
22. Downs JC, Blidner RA, Bellezza AJ, Thompson HW, Hart RT, Burgoyne CF. Peripapillary scleral thickness in perfusion-fixed normal monkey eyes. *Invest Ophthalmol Vis Sci.* 2002;43:2229-2235.
23. Timoshenko S, Goodier JN. *Theory of Elasticity.* New York: McGraw-Hill; 1934.
24. Hernandez MR, Luo XX, Igoe F, Neufeld AH. Extracellular matrix of the human lamina cribrosa. *Am J Ophthalmol.* 1990;109:180-188.
25. Goldbaum MH, Jeng SY, Logemann R, Weinreb RN. The extracellular matrix of the human optic nerve. *Arch Ophthalmol.* 1989;107:1225-1231.
26. Morrison JC, L'Hernault NL, Jerdan JA, Quigley HA. Ultrastructural location of extracellular matrix components in the optic nerve head. *Arch Ophthalmol.* 1989;107:123-129.